Physics – Uspekhi **55** (11) 1115 – 1123 (2012)

INSTRUMENTS AND METHODS OF INVESTIGATION PACS numbers: 42.50.Wk, 42.65.Es, **43.40.+s**, **46.40.–f**

Parametric oscillatory instability in gravitational wave laser detectors

S P Vyatchanin, S E Strigin

DOI: 10.3367/UFNe.0182.201211e.1195

Contents

Abstract. The nonlinear effect of parametric oscillatory instability in the gravitational wave laser detector (antenna) is considered as a factor that considerably reduces the sensitivity of the device. It is shown that in an antenna with a circulating power above a certain threshold value, excitation of Stokes optical modes occurs in Fabry–Perot resonators and of test mass elastic modes. Parametric oscillatory instability in gravitational wave interferometers of the second (LIGO, Virgo, LCGT, GEO-600) and third (ET — Einstein Telescope) generation with different types of pumps is examined. The effect discussed has been observed not only in gravitational wave laser interferometers, but also many times in other opto-mechanical systems. All current methods for suppressing parametric oscillatory instability in gravitational wave interferometers are also discussed, both passive and active.

1. Introduction

The advent of lasers in the 1960s led to the discovery of new phenomena involving molecular light scattering from microscopic inhomogeneities — the spontaneously emerging and vanishing fluctuations of thermodynamic parameters of a medium [1–4]. The parametric oscillatory instability phenomenon under consideration is, by its physical nature, close to the stimulated Mandelstam–Brillouin scattering [5–7] and the stimulated Raman scattering [8] of light.

Stimulated light scattering in a medium is due to nonlinear properties of the medium and is brought about by the incident light wave. In particular, Mandelstam–Brillouin scattering is caused by the interaction of light and elastic (sonic or hypersonic) waves. This effect is easy to interpret in quantum terms: a photon of the incident light (of the laser pump) with frequency ω_0 decays into a photon with a lower frequency $\omega_1 < \omega_0$ (the so-called Stokes wave) and a phonon of the elastic wave with frequency ω_m. As this takes place, the energy conservation law is always satisfied: $\hbar\omega_0 = \hbar\omega_1 + \hbar\omega_m$.

When the incident light intensity is low, the energy reradiated to the Stokes and elastic waves is small. However, wave interaction at the combination frequencies becomes progressively stronger with increasing intensity of the incident light. In particular, the ponderomotive force at the difference frequency $\omega_0 - \omega_1 \simeq \omega_m$ becomes stronger, which acts on the elastic medium and intensifies the generation of elastic waves at the frequency ω_m. On the other hand, the nonlinear interaction of elastic waves with the pump wave enhances the generation of light waves at the Stokes frequency $\omega_1 \simeq \omega_0 - \omega_m$. When the pump power reaches some threshold value, these processes become dominant, which results in a sharp increase in intensity of the scattered radiation, namely in the emergence of stimulated Mandelstam–Brillouin scattering [5–7].

A lucid illustration of the parametric light scattering described above is provided by the model of a two-circuit parametric amplifier (Fig. 1) which consists of two parallel oscillatory circuits connected with a variable coupling capacitance $C_0(t) = C_0 + \delta C \cos\omega_0 t$ [9]. It is commonly known that the operation of the parametric amplifier becomes unstable under sufficiently strong pumping (i.e., for a sufficiently large modulation part δC of the coupling capacitance). For a perfect matching (i.e., when $\omega_0 = \omega_a + \omega_b$), the instability condition is written in the following form:

$$\frac{\delta C^2}{C_a C_b} > \frac{\gamma_a \gamma_b}{\omega_a \omega_b}\,, \quad \gamma_a \equiv \frac{R_a}{2L_a}\,, \quad \gamma_b \equiv \frac{R_b}{2L_b}\,, \tag{1}$$

where R_a and R_b are the resistances, C_a, C_b are the capacitances, and L_a, L_b are the inductances of the circuits, respectively (see the notation in Fig. 1).

It is also well known that parametric pumping introduces *negative* damping (antidamping), and that condition (1) in

S P Vyatchanin, S E Strigin Department of Physics,
M V Lomonosov Moscow State University,
Leninskie gory, 119991 Moscow, Russian Federation
Tel. +7 (495) 939 44 28
E-mail: svyatchanin@phys.msu.ru, strigin@phys.msu.ru

Received 19 March 2012
Uspekhi Fizicheskikh Nauk **182** (11) 1195 – 1204 (2012)
DOI: 10.3367/UFNr.0182.201211e.1195
Translated by E N Ragozin; edited by A Radzig

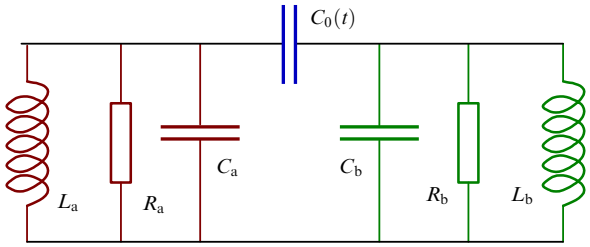

Figure 1. Two-circuit parametric amplifier model. The circuit partial frequencies ω_a, ω_b and the modulation frequency ω_0 of the coupling capacitance $C_0(t) = C_0 + \delta C \cos \omega_0 t$ obey the relationship $\omega_0 \simeq \omega_a + \omega_b$.

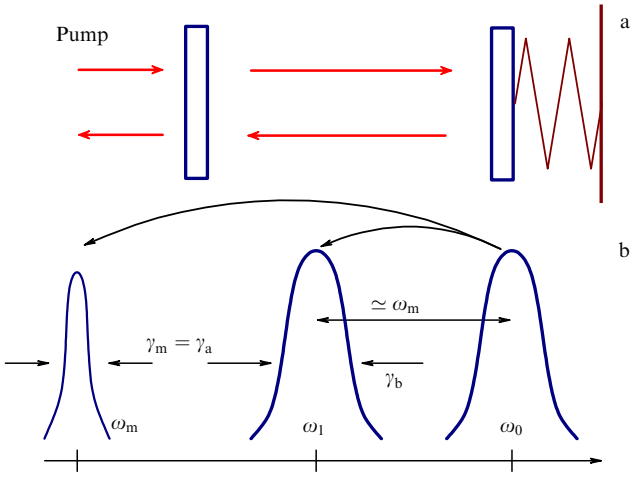

Figure 2. (a) Schematic of a Fabry–Perot cavity in which one of its mirrors is movable and constitutes a mechanical oscillator with frequency ω_m. (b) Mode diagram. The arrows indicate energy fluxes in accordance with Manley–Rowe relations.

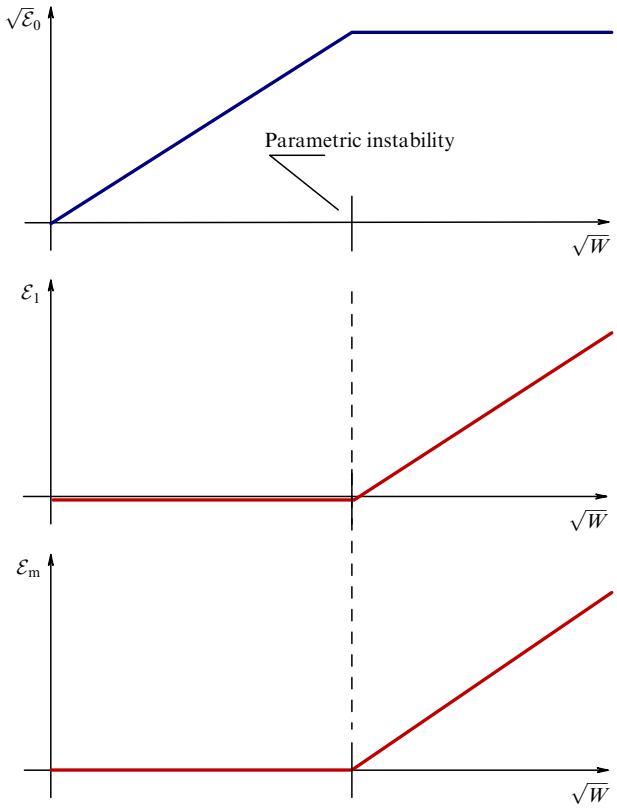

Figure 3. Respective energies $\mathcal{E}_0$, $\mathcal{E}_1$, and $\mathcal{E}_m$ in the fundamental, Stokes, and mechanical modes as functions of the pump power W, below and above the parametric instability threshold.

fact describes a situation wherein the insertion loss becomes stronger than the intrinsic one [10].

The instability condition for the parametric amplifier is quite similar to the condition for the emergence of stimulated Mandelstam–Brillouin scattering, with the Stokes wave associated with the partial mode of frequency ω_a, and the elastic wave associated with the mode of frequency ω_b.

To qualitatively analyze the phenomenon of parametric oscillatory instability (POI), we consider the model of a Fabry–Perot (FP) cavity (Fig. 2) excited by resonant pumping at a frequency ω_0. One of the cavity mirrors is movable and constitutes a mechanical oscillator at the frequency ω_m. Let there be a Stokes optical cavity mode with an eigenfrequency ω_1, so that the following condition is fulfilled:

$$\omega_0 \simeq \omega_1 + \omega_m \,. \tag{2}$$

Parametric interaction between these modes is possible in this case, which may give rise to parametric instability [11–15]. In the presence of small oscillations in the Stokes optical mode, a ponderomotive force emerges at the difference frequency $\omega_0 - \omega_1 \simeq \omega_m$, which acts on a movable mirror and *resonantly* excites mechanical oscillations. On the other hand, the small mechanical oscillations of the mirror give rise owing to the Doppler effect to mirror-reflected waves at the combination frequencies $\omega_0 \pm \omega_m$. One of these waves resonantly excites (at the frequency $\omega_0 - \omega_m \simeq \omega_1$) oscillations in the Stokes optical mode. With increasing pump power at the frequency ω_0, the stated mechanisms will evidently result in progressively greater energy transfer between different waves. In accordance with Manley–Rowe relations, the energy of the pump wave will be transferred to the Stokes optical and mechanical modes. This effect may be treated as the introduction of *antidamping*, and therefore parametric instability will emerge when the pump power reaches some threshold value.

In reality, the role of mechanical oscillator is played by *elastic* oscillation modes in the mirrors, which have different spatial distributions of the components of the elastic displacement vector [16–18]. These modes may be related to the Stokes optical modes with *appropriate* field distributions on the mirror surfaces (for details, see Section 2).

Parametric oscillatory instability can become an unwanted parasitic effect in laser gravitational wave antennas in which it is planned to employ a high circulating light power W [about 830 kW in the Advanced LIGO (Laser Interferometer Gravitational-wave Observatory) interferometer]. Not a few appropriate Stokes and elastic mode pairs may exist for so high a light power value, which will give rise to POI [19–22].

When the condition of POI emergence is fulfilled, a further increase in laser pump power has the effect that the energy $\mathcal{E}_0$ in the fundamental mode at the frequency ω_0 ceases to increase, but the energies in the Stokes and mechanical modes begin to increase [23], as illustrated in Fig. 3. This increase may give the result that the Stokes mode will begin to play the role of a pump for the excitation of the next appropriate Stokes and mechanical mode pair. Therefore, a cascade POI development becomes possible [24, 25].

The POI phenomenon was observed in optical microcavities [26–29] for a modest optical pump power of about 10^{-4} W; this was attributable to the high Q factors (on the order of 10^9) of optical modes and the small mass of mechanical oscillations (about 10^{-10} kg). That is why the cascade POI is relatively easy to obtain in such microcavities. This makes possible the generation of optical combs [30–33].

It should be emphasized that an appropriate optical *anti-Stokes* mode with a frequency $\omega_{1a} \simeq \omega_0 + \omega_m$ may also exist in the cavity. In this case, in accordance with the Manley–Rowe relations, the pump will introduce *positive* damping into the mechanical mode, which may be stronger than the negative damping introduced by the Stokes mode, so that parametric instability will be impossible. In this case, a pump wave photon is scattered by an elastic photon to produce an anti-Stokes wave photon, and a part of the energy is taken from the elastic wave. That is why, on the one hand, the presence of the Stokes optical mode introduces anti-damping into the mechanical mode (and hence to the parametric instability effect) and, on the other hand, the presence of the anti-Stokes mode results in the damping of the mechanical mode [34, 35]. However, the probability that the anti-Stokes modes will completely suppress the parametric instability is quite low [12, 36].

The layout of the paper is as follows. We consider the possibility of POI emergence in a Fabry–Perot (FP) cavity in Section 2, and in second-generation gravitational wave interferometers [LIGO, Virgo, LCGT (Large-scale Cryogenic Gravitational-wave Telescope), GEO-600] and in the third-generation interferometer (Einstein Telescope, ET) in Section 3. Section 4 concerns the influence of different shapes of the laser pump beam on the likelihood of POI. No less important are the problems of suppression of the parametric instability and its experimental verification, which are the concern of Sections 5 and 6. Also considered in Section 6 are other optomechanical systems in which the parametric instability can manifest itself.

2. Parametric instability in a Fabry–Perot cavity

The POI phenomenon and its emergence condition in a single FP cavity were first considered in detail in Ref. [11] on the basis of the simple model depicted in Fig. 2. This model proposes the interaction of only two modes — a Stokes optical mode with frequency ω_1, and one of the elastic modes of the mirror (probe mass) with frequency ω_m. In this case, one of the cavity mirrors (the right one in Fig. 2a) may be treated as a mechanical oscillator. These modes interact due to the high power in the fundamental mode with frequency ω_0, which is assumed to be given (a given pump approximation). It is also assumed that the frequencies ω_0, ω_1, and ω_m approximately satisfy condition (2). Then, the POI condition for the FP cavity may be expressed as [11]

$$\mathcal{R} = \frac{W\omega_1}{cLm\omega_m\gamma_1\gamma_m}\,\frac{\Lambda_1}{1+(\Delta_1/\gamma_1)^2} > 1\,, \tag{3}$$

$$\Lambda_1 \equiv \frac{V\left|\int \mathcal{A}_0\mathcal{A}_s^* u_z\,\mathrm{d}\mathbf{r}_\perp\right|^2}{\int|\mathcal{A}_0|^2\,\mathrm{d}\mathbf{r}_\perp\int|\mathcal{A}_s|^2\,\mathrm{d}\mathbf{r}_\perp\int|\mathbf{u}(\mathbf{r})|^2\,\mathrm{d}\mathbf{r}}\,, \tag{4}$$

$$\Delta_1 = \omega_0 - \omega_1 - \omega_m\,, \tag{5}$$

where W is the light power circulating in the fundamental mode of the FP cavity, γ_1, γ_m are the damping coefficients for the Stokes optical and elastic modes, L is the separation between the FP cavity mirrors, c is the speed of light, m is the mirror mass, Δ_1 is the frequency mismatch, Λ_1 is the overlap ratio for the distributions of fundamental, Stokes optical, and elastic modes, $\mathcal{A}_0$, $\mathcal{A}_s$ are the light field distribution functions over the beam cross section for the fundamental and Stokes modes, u_z is the component of the displacement vector $\mathbf{u}$ for the elastic mode perpendicular to the base surface of the cylindrical mirror, integration with respect to $\mathrm{d}\mathbf{r}_\perp$ corresponds to integration over the mirror surface, and integration with respect to $\mathrm{d}\mathbf{r}$ corresponds to integration over the mirror volume V.

At a given pump frequency ω_0, it is necessary to analyze all appropriate combinations of Stokes and elastic modes that satisfy condition (2) and to check whether condition (3) is fulfilled for them. Evidently, the number of such pairs can be relatively large. While the eigenfrequencies and optical mode distributions in an FP cavity with spherical mirrors can be written in an analytical form, the mirror elastic modes have to be calculated numerically. Fortunately, for a cavity with mirrors of *finite* size, the diffraction losses for the optical modes increase with mode order (this signifies an increase in optical damping γ_1), and so the number of the optical modes being calculated is limited. We note that the frequencies ω_m of the elastic modes of FP cavity mirrors are comparable to an order of magnitude with the main intermode spacing $\Delta\omega_{fsr} = \pi c/L \approx 2\times10^5\ \mathrm{s}^{-1}$ in the cavity (see Table 1), which favors the fulfillment of condition (2).

Generally, the possible effect of the anti-Stokes optical mode in the FP cavity should also be taken into account. In view of this requirement, the POI emergence condition takes on the form

$$\mathcal{R} = \frac{W\omega_1}{cLm\omega_m\gamma_1\gamma_m}\,\frac{\Lambda_1}{1+(\Delta_1/\gamma_1)^2} - \frac{W\omega_1}{cLm\omega_m\gamma_1\gamma_m}\,\frac{\omega_{1a}\gamma_1}{\omega_1\gamma_{1a}}\,\frac{\Lambda_{1a}}{1+(\Delta_{1a}/\gamma_{1a})^2} > 1\,, \tag{6}$$

$$\Lambda_{1a} \equiv \frac{V\left|\int \mathcal{A}_0\mathcal{A}_{as}^* u_z\,\mathrm{d}\mathbf{r}_\perp\right|^2}{\int|\mathcal{A}_0|^2\,\mathrm{d}\mathbf{r}_\perp\int|\mathcal{A}_{as}|^2\,\mathrm{d}\mathbf{r}_\perp\int|\mathbf{u}(\mathbf{r})|^2\,\mathrm{d}\mathbf{r}}\,, \tag{7}$$

$$\Delta_{1a} = \omega_{1a} - \omega_0 - \omega_m\,, \tag{8}$$

where γ_{1a} is the damping coefficient of the anti-Stokes optical mode, and $\mathcal{A}_{as}$ is the light field distribution function over the beam cross section of the anti-Stokes mode.

The second term in the right-hand side of formula (6) takes into account the possible influence of the anti-Stokes mode. It is evident that a combination of parameters is possible, such that the second term will compensate for the

Table 1. Parameters of the Fabry–Perot cavity for the Advanced LIGO interferometer.

Power W	0.83×10^6 W
Length L	4000 m
Mirror mass m	40 kg
Mirror radius R	0.17 m
Mirror thickness H	0.2 m
Material	Fused quartz

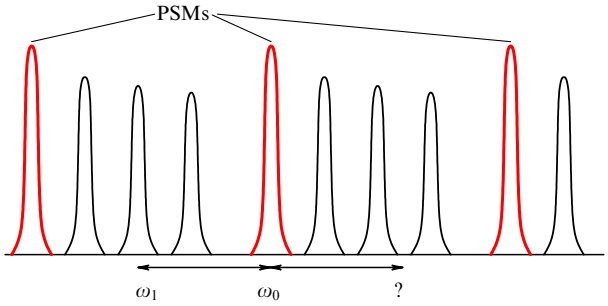

Figure 4. Structure of the optical FP cavity modes. The principal sequence modes (PSMs) correspond to high peaks. The Stokes optical mode has a frequency ω_1, and the possible anti-Stokes mode is labelled by a question mark.

first term (the positive damping which the anti-Stokes mode introduces into the elastic mode exceeds the negative damping caused by the Stokes mode), and then the POI effect will be suppressed [34, 35]. For instance, let us assume that the fundamental, Stokes, and anti-Stokes modes are equidistant: $\omega_1 = \pi(K-1)\,c/L$, $\omega_0 = \pi Kc/L$, $\omega_{1a} = \pi(K+1)\,c/L$ (K is some integer), and have a Gaussian field distribution over the beam cross section. In this case, $\Lambda_1 = \Lambda_{1a}$, $\Lambda_1 = \Lambda_{1a}$, and POI is impossible. However, this kind of mode arrangement is highly unlikely and is of minor significance in finding unstable mode combinations, as illustrated in Fig. 4.

It should be noted that predicting unstable mode combinations requires complete information both about elastic modes and about Stokes optical modes. The frequencies and optical field distributions over the mirror surfaces are readily calculated by analytical techniques for the Gaussian modes of a Fabry–Perot resonator [37], while the frequencies and displacement vector distributions for elastic modes can be found only by numerical simulations. The most popular technique of finding the frequencies and the mode distributions is the finite-difference method (the system of finite-difference elasticity equations is solved for a cylinder).

Also worthy of mention is the superposition method as applied to the axisymmetric elastic modes of a cylindrical mirror [18], which permits obtaining accurately the eigenfrequencies and displacement vector distributions for these modes. Analytical expressions for displacement vector components are constructed using the superposition of the particular solutions of the equation of elastic medium motion subject to zero boundary conditions for the stress on the mirror surfaces [38–43]. This method necessitates moderate computational capacities but, unfortunately, so far it is applicable only to axisymmetric modes.

As discussed above, the finite-difference method is the main technique of obtaining the complete frequency spectrum and the displacement vector distributions for elastic modes necessary in calculating parametric instabilities. However, making exact predictions of these instabilities requires obtaining the numerical solutions with a high accuracy. One can see from condition (3) that the elastic mode eigenfrequencies must be calculated with an error lower than the damping coefficient of the Stokes optical mode. For typical mechanical frequency values ranging from 10 to 100 kHz and an optical relaxation time corresponding to an interval of 10–100 Hz, this signifies that the relative accuracy of the numerical calculation of elastic mode frequencies must be not worse than 10^{-4}. This requirement is not always met in the calculation of elastic modes using, for instance, the COMSOL or ANSYS numerical packages. For example, when use was made of ANSYS, the accuracy of elastic mode calculation was about 0.5% [13–15, 21], and this accuracy is not always sufficient.

Among other physical factors that limit the predicted accuracy of elastic mode frequencies are inhomogeneities in the distributions of the density and Young modulus of the mirror material, which may be responsible for relative shifts of elastic mode frequencies at a level of 10^{-3} [12].

We note that LIGO interferometer mirrors depart slightly from a cylindrical shape due to the plane cuts on the side mirror surface made for the mirror mounts and due to the mounts themselves. These departures will result in altering the frequencies of elastic modes, remove their frequency degeneracy, and split the spectrum of nonaxisymmetric elastic modes into doublets [16, 17]. This is attributable to the fact that modes with the $\sin(m\varphi)$ and $\cos(m\varphi)$ dependences (where m, φ are the azimuthal number and the angle, respectively) must have different frequencies due to different values of the elastic energy of these modes in the domains close to the plane cuts. By contrast, axisymmetric modes do not split, but their eigenfrequencies change. The splitting of the elastic modes will, in turn, raise the POI probability.

An additional azimuthal condition should also be fulfilled for POI prediction. Assume, for instance, that the fundamental pump mode has a Gaussian shape (TEM_{00}), while the elastic and Stokes optical modes have respective azimuthal dependences $\exp(im\varphi)$ and $\exp(in\varphi)$. Then, the mode overlap ratio will be nonzero only when $m=n$ [see formula (4)]. However, this is true only when the center of the cylindrical mirror coincides with the center of the laser beam. In general, there is always a separation Z of the mirror center from the optical mode distribution center. This is due to the fact that the FP cavity mirrors of gravitational detectors may be slightly displaced in space relative to the average position. Consequently, in this case the overlap ratio will depend on the separation Z. For instance, the overlap ratio Λ_1 may become nonzero for $Z \neq 0$, although it is equal to zero at $Z = 0$. This may result in an increase in the number of parametric instabilities developed in the system.

The data of numerical simulations suggest that a mirror displacement $Z = 1$ cm for the Advanced LIGO configuration increases the number of parametric instabilities by approximately 15% [44]. For displacements $Z = 1$ mm expected in Advanced LIGO, the mirror displacement effect does not lead to an increase in parametric instabilities, and the system remains stable.

3. Parametric instability in gravitational wave interferometers

To date, several laboratories in the world have demonstrated the operation of first-generation gravitational wave laser detectors (LIGO [45, 46], Virgo [47, 48], GEO-600 [49, 50], and TAMA [50, 51] projects), and work is already underway to develop second-generation detectors (Advanced LIGO, Advanced Virgo, GEO-HF, etc.) which will make it possible to detect gravitational waves in the near future. In second-generation detectors, it is planned to substantially increase the light power circulating in interferometer arms (up to 800 kW in Advanced LIGO) [45, 46, 53]. The likelihood of POI in the second-generation gravitational laser detectors will therefore be rather high.

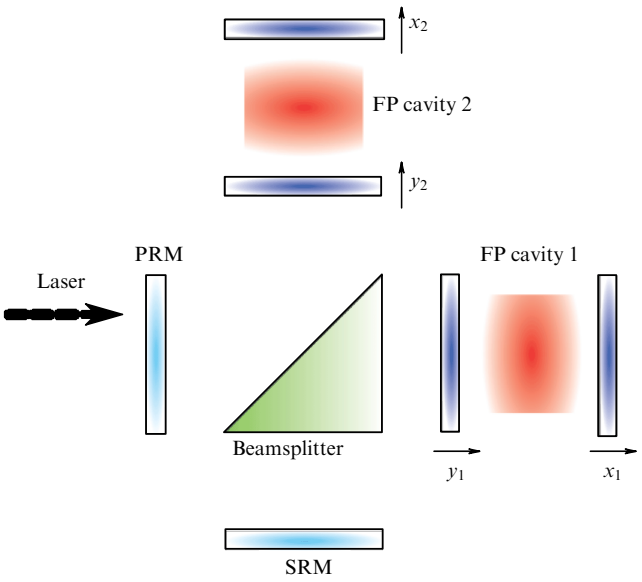

Figure 5. Schematic of the Advanced LIGO interferometer with Fabry–Perot cavities in its arms and with power and signal recycling mirrors (PRM and SRM, respectively).

A simplified layout of the Advanced LIGO interferometer is depicted in Fig. 5. Two cylindrically shaped mirrors suspended at a long distance from each other make up cavity 1 in one Fabry–Perot interferometer arm, while two other similar mirrors make up the second arm with Fabry–Perot cavity 2, which is perpendicular to the first one. The pump laser beam passes through a beamsplitter located at the point of intersection of the arm's lines. It is implied that the light experiences multiple reflections from the mirrors inside each arm before it returns to the beamsplitter. The interferometer arms are aligned in such a way that the entire reflected light is directed back to the laser (the so-called bright port) and light does not arrive at the detector port (the so-called dark port). Under the action of a gravitational wave, some difference appears between the lengths of the two arm, and a portion of the light propagates to the dark port and is recorded by a photodetector.

The action of a gravitational wave is extremely weak: the Advanced LIGO interferometer is assumed to record a differential displacement on the order of $10^{-17}-10^{-16}$ cm in a time of $\sim 10^{-2}$ s for an arm length of 4 km. Detection of so small a displacement implies that the mirror displacements caused by other reasons — thermal, seismic, and technical noise [54–62] — are extremely small. Even an insignificant displacement of the mirrors has the effect that the beams arrive at the beamsplitter with altered phases and thereby simulate the detection of a gravitational wave.

In the improved Advanced LIGO interferometer, two additional mirrors — a power recycling mirror (PRM), and a signal recycling mirror (SRM) — are introduced into the standard Michelson scheme with FP cavities in its arms (see Fig. 5). The former mirror is employed only for increasing the circulating power: with the same pump laser, the light energy inside an interferometer arm will be $\sim T^{-2}$ times higher in the scheme with a PRM, where T is the amplitude PRM transmission coefficient, other parameters of the system being the same.

As shown in Ref. [12], the presence of a PRM increases the probability of a POI emergence in comparison with that in the case of a single FP cavity. This is attributable to the fact that the Stokes mode emitted from the FP cavity 1 through its input mirror is not irrevocably lost but returns to the cavity owing to the presence of PRM, and its interaction with elastic modes will therefore continue. For instance, the presence of the cavity with the PRM significantly increases the value of $\mathcal{R}$ for a zero mismatch Δ_1 (resonance), and lowers $\mathcal{R}$ by about a factor of two away from the resonance in comparison with the case without the PRM [21].

A series of papers [19, 20, 63] were concerned with the analysis of POI in the Advanced LIGO interferometer in the presence of an SRM. When considering parametric instability, it was convenient to introduce the so-called sum and difference optical modes, which are the sum and difference of the light fields in the interferometer arms. The sum optical mode will interact with the sum elastic mode, $z_+ = (x_1 - y_1) + (x_2 - y_2)$, and the difference optical mode will interact with the difference elastic mode, $z_- = (x_1 - y_1) - (x_2 - y_2)$, where x_i, y_i $(i = 1, 2)$ are the mirror coordinates in the interferometer arms (see Fig. 5). We emphasize that this assumption is likely when all four mirrors of the FP cavities are identical.

It was shown that the POI in the Advanced LIGO interferometer with an additional SRM may, on the one hand, emerge at relatively low values of the pump power circulating in the interferometer arms (on the order of several watts) but, on the other hand, the probability that the POI condition is fulfilled is extremely low because of the small value of the optical mode damping coefficient, $\gamma_1 \simeq 2\ \mathrm{s}^{-1}$ [see formula (3)]. A comprehensive analysis of POI in the presence of both an SRM and a PRM is given in Refs [22, 64].

The problem of emerging parametric instability in the second-generation European antenna, termed Advanced Virgo, is about the same as in Advanced LIGO because so far they have had close parameters [48].

The Japan LCGT antenna now under construction, which has approximately the same dimensions (an arm length of 3 km) as Advanced LIGO and Advanced Virgo, has two essential distinctions from them: it should operate at cryogenic temperature (20 K), and its mirrors are planned to be made of sapphire (sapphire at low temperatures provides substantially lower losses than fused quartz). From the POI standpoint, the LCGT antenna offers several advantages: a more sparse spectrum of elastic modes (the sound velocity in sapphire is nearly two times higher than in fused quartz), and a more sparse spectrum of optical modes [owing to the employment of mirrors with a longer radius of curvature (over 7 km)]. Estimates show [65] that the number of mode combinations harmful from the POI standpoint is approximately ten times smaller in LCGT (2–4) than in Advanced LIGO (20–60) [14]. This provides a way of suppressing the POI by introducing additional damping via the feedback loop.

Apart from the 'large' antennas mentioned above, two somewhat smaller antennas are being operated today: the German–British GEO-600 [49] (with an arm of 600 m), and the Japanese TAMA-300 [51] (with a 300-m arm). Owing to the lower light power circulating inside these antennas, the probability of a POI emergence is low; however, they may be employed for the observation of POI and its precursors in order to develop technologies for POI suppression [66].

At present, the European Gravitational Observatory is developing the project of a third-generation gravitational wave interferometer named the Einstein Telescope (ET). It is expected that the ET will outperform second-generation gravitational wave detectors by several orders of magnitude in sensitivity [67, 68]. The details of this project are at the

development stage, but the first data about the parameters of the FP cavities that make up the ET arms have been indicated in Ref. [68].

The light power circulating in the FP cavities of the Einstein Telescope will amount to 3 MW, which will promote a substantial improvement in detector sensitivity. However, the probability of POI will also rise at the same time [see formula (6)]. Also, the separation of FP cavity mirrors will be increased to 10 km, the radius of the laser beam on the mirrors will lengthen to 12 cm, and the previous room-temperature detector operation mode will be replaced with operation at a temperature of about 20 K, which will diminish the effect of different kinds of thermal noise. It is suggested that the mirror radius will be increased to 30 cm, which is approximately 2.5 times greater than the radius of the laser beam on the mirrors, and therefore diffraction losses of the optical pump mode will be extremely low (3.7 ppm). To lower the level of seismic influence, it is planned to accommodate the ET in a horizontal tunnel located underground at a depth of about 800 m [67, 68].

The calculation of POI for the Einstein Telescope was made for the elastic modes of fused quartz mirrors in a frequency range of up to 30 kHz [69]. The resultant number of unstable modes (five modes in the specified frequency interval) is comparable to the number of instabilities for the Advanced LIGO interferometer. Also considered were two possible Einstein Telescope configurations with FP cavity mirrors made of silicon and sapphire [70]. In this case, the number of unstable modes in the Einstein Telescope exceeds the number of POI-unstable modes for the Advanced LIGO interferometer (eight unstable combinations for sapphire mirrors and twelve combinations for silicon ones were discovered in an elastic mode frequency range of up to 40 kHz). This fact is attributable to the higher spectral density of elastic mirror modes and optical modes.

4. Effect of different pump types (TEM_{00}, LG_{33}, and mesa modes)

The most important problem encounted in searching for gravitational waves consists in weakening the influence of fundamental and technical noise in gravitational wave interferometers on the antenna sensitivity. One way to weaken this influence is to change the shape of the laser pump beam inside the interferometer. It is noteworthy that different pump mode shapes have been proposed for lowering, for instance, thermal noise: so-called mesa beams [71–73], conical modes [74], and high-order Laguerre–Gauss modes [75]. At present there are several methods of generating high-order Laguerre–Gauss (LG) modes with the use of holograms [76, 77], diffraction gratings [78], and different mode converters with a high efficiency [78, 81]. An LG_{33} optical pump mode (a possible candidate for the role of a pump mode in gravitational wave interferometers) was compared with a TEM_{00} Gaussian pump mode in Ref. [82]. It is pertinent to note that the LG_{33} pump mode proved to be even better suited in terms of many characteristics (immunity to small rotations and displacements of the mirrors, diffraction losses, etc.) than the TEM_{00} mode [82].

The number of unstable combinations of elastic and Stokes modes in the cases of TEM_{00} and LG_{33} mode pumping was calculated in Ref. [83]. In the elastic mode frequency interval (up to 40 kHz) investigated, the probability of the emergence of POI in the case of an LG_{33} type pump

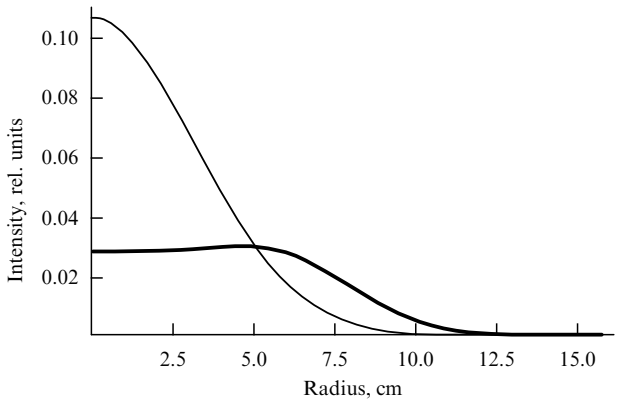

Figure 6. Intensity distributions in a Gaussian light beam (mode) of radius $r_0 = 4.5$ cm for cylindrical mirrors of radius $R = 15.7$ cm (thin curve) and in a mesa light beam of radius 9.71 cm for similar cylindrical mirrors of radius $R = 15.7$ cm (bold curve). The level of diffraction loss per reflection from a probe mass is equal to 10 ppm [71, 72].

turned out to be somewhat higher than in the case of a TEM_{00} pump for the Advanced LIGO interferometer. However, the difference in the number of unstable modes in these two cases is not large enough to unambiguously state that the LG_{33} pump is less safe than the TEM_{00} pump from the POI standpoint.

Earlier, it was planned to employ light beams with a flat top, long radius, and steep 'edges' instead of Gaussian beams with a small radius and gently sloping edges [71–73]. Since the intensity distribution in these beams resembles a mesa — a flat tableland with steep edges, common in the southwestern US desert — they have come to be known as mesa beams. Figure 6 depicts the intensity distributions for the proposed mesa beam (bold line) and the intensity distribution of the Gaussian beam (thin line) with the similar levels of diffraction losses.

When comparing mesa beams and a Gaussian mode as pump waves, it was found that the mode overlap factors for 70% of elastic modes have higher values in interferometer cavities that support mesa modes [84]. At the same time, owing to their rapidly decreasing light field distributions, the mesa modes have low diffraction losses in comparison with those for Gaussian modes (lower by an order of magnitude). The structure of optical modes in FP cavities that support mesa mode propagation is also different from the Gaussian mode structure, which will necessarily manifest itself in the POI effect.

These three factors — the difference in cavity optical mode structure, low diffraction losses, and large overlap factors — have a strong influence on POI. An analysis suggests that the number of unstable combinations of elastic and Stokes optical modes rises by about a factor of three when use is made of mesa beams as pump waves in lieu of Gaussian beams [84]. At the same time, the average value of parameter $\mathcal{R}$ is somewhat smaller. Therefore, POI will show its worth somewhat more strongly when advantage is taken of the mesa beams instead of the Gaussian pump mode.

5. Methods for parametric instability suppression

Parametric oscillatory instability in gravitational wave laser antennas may be responsible for a considerable lowering of their sensitivity in the detection of gravitational waves, and

the development of efficient POI suppression methods is, therefore, a burning problem. Today, there are three main ways of suppressing the POI:

• changing the radius of curvature of mirrors by their thermal heating (for instance, using an additional laser beam) [13, 64, 85];

• lowering the Q factor of mechanical modes [21, 64, 86];

• introducing additional damping into 'dangerous' elastic modes with the aid of electrostatic feedback forces [87].

The emergence probability of unstable POI modes and their number depend heavily on the radius of curvature of interferometer mirrors (the mismatch Δ between the modes is determined by these radii). The radii of mirror curvature are not fixed interferometer parameters and they can be changed, for instance, by the thermal heating of the mirrors, i.e., due to the thermal lensing effect [13, 64, 85]. Since the radii of mirror curvature define the magnitudes of the mode mismatch Δ and, hence, the $\mathcal{R}$ parameter values for the combinations of optical and mechanical modes, there are optimal values of these radii whereby the number of unstable modes decreases in comparison with that in the standard interferometer configuration.

The second efficient way of suppressing POI consists in the lowering of the Q factor of mechanical mirror modes by depositing annular strips onto the side cylindrical surface of the mirrors with the application of copper or gold ion deposition technology. The mechanical properties of these strips are hardly different from those of the material the mirror is made of. The deposition of an annular strip (for instance, 20 μm in thickness [21]) onto the side mirror surface will result not only in a lowering of the Q factor of mechanical mirror modes, but also in an increase in the noise level of thermal origin (in accordance with the fluctuation-dissipative theorem). Evidently, it is most logical that the strip should be located in the region wherein the elastic energy of a unit volume of low-frequency modes is minimum, so as to minimize the adverse effect arising from the emergence of additional thermal noise. It was shown in Refs [21, 64, 86] that the minimum of elastic energy is located virtually in the middle of the side mirror surface. Depositing the strip (loss angle of the strip material is $\phi = 3.6 \times 10^{-3}$, and the strip width is 3 cm) onto this surface area results in an increase in the level of thermal noise in the interferometer by only 5%, which permits the Q factor of mechanical modes to be optimally lowered without a large increase in the contribution from thermal noise. Such an approach, in turn, also permits lowering the $\mathcal{R}$ value for many combinations of optical and mechanical modes. This all may weaken the effect of POI to an acceptable level whereat the interferometer becomes stable.

Recently, a new method was proposed for the active suppression of instabilities, which involves application of forces of electrostatic origin to plane surfaces of interferometer mirrors [87]. In the gravitational wave detectors of Advanced LIGO, use will be made of a system of electrodes located symmetrically near the mirror surface in order to electrostatically control the position of suspended interferometer mirrors. The potential difference between the electrodes and the plane mirror surface gives rise to electrostatic forces which act on the dielectric mirrors and control their position. This brings up the natural idea of using these forces for introducing additional damping into the mechanical degrees of freedom of mirrors and lowering their Q factor (at the frequencies of elastic modes). At first, the authors of Ref. [87] theoretically calculated the magnitudes of forces required to suppress parametric instabilities in gravitational wave antennas and experimentally confirmed the results of their calculations. They next reached a conclusion that the use of electrostatic forces in the system facilitates controling the number of parametric instabilities. Similar ideas of active POI suppression had earlier been advanced in Ref. [88].

The authors of Refs [14, 64, 85, 86] also proposed the utilization of other materials for interferometer mirror fabrication, as a method of lowering the emergence probability of POI. Sapphire is regarded as the most acceptable candidate for the mirror material: owing to its mechanical properties, sapphire has a relatively low density of elastic mechanical modes, which can minimize the emergence probability of parametric instability and the number of unstable modes. However, the final decision about the use of sapphire as the material for interferometer mirrors has not been made, because there are several problems associated with the employment of sapphire in interferometers, like its anisotropic properties and some others.

It is pertinent to note that none of the POI suppression techniques described above ensures complete elimination of POI. However, by combining the methods of instability suppression, in all likelihood it will be possible to achieve success with different schemes of gravitational wave interferometers.

6. Experimental verification

Theoretical predictions of the emergence of POI in gravitational wave interferometers or other optomechanical systems call for an undelayable experimental verification in order to understand the true scale of the danger facing the developers of new-generation interferometers. The first attempts to experimentally reveal the three-mode interaction were undertaken in Ref. [89], where the fundamental optical pump mode and the anti-Stokes first-order transverse TEM_{01} mode of an FP cavity interacted with a low-frequency mechanical mirror mode. The energy of the fundamental pump mode was reradiated to the anti-Stokes mode due to its interaction with the mechanical mirror mode at a frequency of 158.11 kHz. This experiment was carried out using a 77-m-long FP cavity with sapphire mirrors, with a light power of 1 kW circulating in the cavity. This experiment does not explicitly demonstrate the POI effect: it merely confirms the interaction between the fundamental optical pump mode and the anti-Stokes mode, which results in the damping of mechanical oscillations.

It should be noted that the three-mode interaction may be experimentally discovered by observing the amplitude of either the mechanical mode or the anti-Stokes optical mode. The experiment of Ref. [89] involved power measurements of the anti-Stokes optical TEM_{01} mode as a function of the frequency difference between the anti-Stokes and fundamental pump modes. It was found that the resonance interaction between the FP cavity optical and mechanical modes appears when the frequency separation of two optical cavity modes is close to the frequency of a mechanical mirror mode. These experimental results are in perfect agreement with theoretical predictions [formula (6)], which allows the conclusion that the POI effect may take place in future schemes of third-generation gravitational wave antennas.

Parametric instability has also been observed on a microscale — in the whispering gallery modes of toroidal microcavities. A toroid of fused quartz (several micrometers high, and 50–100 μm in diameter) constitutes an optical

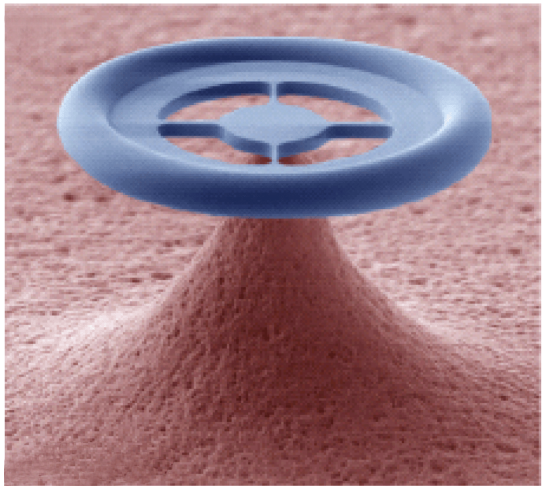

Figure 7. Toroidal microcavity (photograph borrowed from http://k-lab.epfl.ch/).

cavity in which a light wave 'describes circles' inside the toroid. The toroid is affixed to its base with a thin membrane or straps (Fig. 7). The frequency of mechanical toroid oscillations (bending and tension) lies in the range from 1 to 100 MHz. These oscillations change the optical path of light in the cavity, thereby establishing optomechanical mode coupling (for details see Ref. [90]). Owing to the small dimensions of these cavities, POI is observed in them for a moderate optical pump power, from several to several hundred microwatts [26, 28]. The optomechanical coupling turns out to be rather strong: it has been possible to measure mechanical shifts with an uncertainty of about 10^{-19} m $\mathrm{Hz}^{-1/2}$ [90]. Additional information can be found in a comprehensive review [91].

It is worthy of note that there is a plethora of optomechanical interaction mechanisms, apart from the mechanism mentioned above. In particular, interesting results were recently obtained using the interaction of light with surface acoustic waves in whispering gallery microcavities [92–94].

7. Conclusions

Parametric oscillatory instability will play an important role not only in presently existing second-generation gravitational wave antennas (like LIGO and Virgo), but also in the third-generation gravitational wave antenna scheme — the ET — being designed. The solution to the problem of gravitational wave detection requires an extremely high accuracy of the measurement of probe mass shifts, and a high sensitivity of gravitational wave detectors. POI, in turn, may be responsible for a lowering of antenna sensitivity and may make impossible the detection of FP cavity mirror shifts caused by the arrival of gravitational waves. However, it is hoped that the passive and active methods of POI suppression developed to date will be able to neutralize its adverse effect on the sensitivity of gravitational wave antennas.

In summary, it is worth pointing out the most radical way of POI control — the lowering of the optical power circulating in interferometer arms. And this is possible in principle. The point is that the second-generation gravitational wave antennas are supposed to reach the measurement accuracy close to the standard quantum limit [10] at frequencies of about 100 Hz. This frequency is defined by the quality of isolation from seismic noise. It is significant that the requisite optical power is proportional to the *third power* of the frequency. Therefore, if attempts to move from a frequency of 100 Hz to a frequency of 30 Hz meet with success, the circulating power will be significantly lower: instead of 800-kW power, it will be sufficient to have a power of about 20 kW (at present, this possibility is discussed theoretically, for instance, for the ET). Furthermore, the intensity of gravitational radiation is expected to be higher in the lower-frequency region. At present, however, everything is hampered by the quality of isolation from seismic noise.

Acknowledgments. The authors express their appreciation to the Russian Foundation for Basic Research (grants Nos 08-02-00580-a and 11-02-00383-a) and the U.S. National Science Foundation (grant PHY-0967049). This work was also supported by a grant from the President of the Russian Federation (MK-195.2007.2), grants from Lomonosov Moscow State University (2008, 2009, 2011, and 2012), and grants from the Dynasty Foundation (2006–2011).

References

1. Fabelinskii I L *Molekulyarnoe Rasseyanie Sveta* (Molecular Scattering of Light) (Moscow: Nauka, 1965) [Translated into English (New York: Plenum Press, 1968)]
2. Starunov V S, Fabelinskii I L *Usp. Fiz. Nauk* **98** 441 (1969) [*Sov. Phys. Usp.* **13** 428 (1970)]
3. Fabelinskii I L *Usp. Fiz. Nauk* **164** 897 (1994) [*Phys. Usp.* **37** 821 (1994)]
4. Fabelinskii I L *Usp. Fiz. Nauk* **168** 1341 (1998) [*Phys. Usp.* **41** 1229 (1998)]
5. Mandelstam L I *Zh. Russk. Fiz.-Khim. Obshchestva Ch. Fiz.* **58** 381 (1926)
6. Brillouin L *Ann. Physique* **17** 88 (1922)
7. Chiao R Y, Townes C H, Stoicheff B P *Phys. Rev. Lett.* **12** 592 (1964)
8. Woodbury E I, Ng W K *Proc. IRE* **50** 2367 (1962)
9. Migulin V V et al. *Osnovy Teorii Kolebanii* (Basic Theory of Oscillations) (Moscow: Nauka, 1978) [Translated into English (Moscow: Mir, 1983)]
10. Braginsky V B *Fizicheskie Eksperimenty s Probnymi Telami* (Physical Experiments with Probe Bodies) (Moscow: Nauka, 1970)
11. Braginsky V B, Strigin S E, Vyatchanin S P *Phys. Lett. A* **287** 331 (2001)
12. Braginsky V B, Strigin S E, Vyatchanin S P *Phys. Lett. A* **305** 111 (2002)
13. Zhao C et al. *Phys. Rev. Lett.* **94** 121102 (2005)
14. Ju L et al. *Phys. Lett. A* **355** 419 (2006)
15. Ju L et al. *Phys. Lett. A* **354** 360 (2006)
16. Strigin S E, Blair D G, Gras S, Vyatchanin S P *Phys. Lett. A* **372** 5727 (2008)
17. Strigin S E *Phys. Lett. A* **372** 6305 (2008)
18. Meleshko V V, Strigin S E, Yakymenko M S *Phys. Lett. A* **373** 3701 (2009)
19. Strigin S E, Vyatchanin S P *Phys. Lett. A* **365** 10 (2007)
20. Vyatchanin S P, Strigin S E *Kvantovaya Elektron.* **37** 1097 (2007) [*Quantum Electron.* **37** 1097 (2007)]
21. Gras S, Blair D G, Zhao C *Class. Quantum Grav.* **26** 135012 (2009)
22. Evans M, Barsotti L, Fritschel P *Phys. Lett. A* **374** 665 (2010)
23. Polyakov I A, Vyatchanin S P *Phys. Lett. A* **368** 423 (2007)
24. Bahrampour A R et al *Phys. Lett. A* **372** 6298 (2008)
25. Abdi M, Bahrampour A R *Phys. Scripta* **83** 045401 (2011)
26. Kippenberg T J et al. *Phys. Rev. Lett.* **95** 033901 (2005)
27. Matsko A B et al. *Phys. Rev. A* **71** 033804 (2005)
28. Rokhsari H et al. *Opt. Express* **13** 5293 (2005)
29. Grudinin I S, Matsko A B, Maleki L *Phys. Rev. Lett.* **102** 043902 (2009)
30. Savchenkov A A et al. *Phys. Rev. Lett.* **101** 093902 (2008)
31. Grudinin I S, Yu N, Maleki L *Opt. Lett.* **34** 878 (2009)

32. Del'Haye P et al. *Nature Photon*. **3** 529 (2009)
33. Kippenberg T J, Holzwarth R, Diddams S A *Science* **332** 555 (2011)
34. Kells W, D'Ambrosio E *Phys. Lett. A* **299** 326 (2002)
35. Matsko A B et al. *Phys. Rev. A* **66** 043814 (2002)
36. Matsko A B et al. *Opt. Express* **15** 17401 (2007)
37. Kogelnik H, Li T *Appl. Opt*. **5** 1550 (1966)
38. Grinchenko V T, Meleshko V V *Garmonicheskie Kolebaniya i Volny v Uprugikh Telakh* (Harmonic Oscillations and Waves in Solids) (Kiev: Nauk. Dumka, 1981)
39. Hutchinson J R *J. Acoust. Soc. Am*. **51** 233 (1972)
40. Grinchenko V T, Meleshko V V *Sov. Appl. Mech*. **12** 1251 (1976)
41. Grinchenko V T, Meleshko V V *Sov. Phys. Acoust*. **24** 488 (1978)
42. Grinchenko V T, Meleshko V V *Sov. Appl. Mech*. **15** 451 (1979)
43. Hutchinson J R *J. Appl. Mech*. **47** 901 (1980)
44. Heinert D, Strigin S E *Phys. Lett. A* **375** 3804 (2011)
45. Abramovici A et al. *Science* **256** 325 (1992)
46. Sigg D et al. (for the LIGO Scientific Collab.) *Class. Quantum Grav*. **25** 114041 (2008)
47. Acernese F et al. *Class. Quantum Grav*. **25** 114045 (2008)
48. Virgo, http://www.virgo.infn.it
49. Grote H (for the LIGO Scientific Collab.) *Class. Quantum Grav*. **25** 114043 (2008)
50. GEO-600, http://www.geo600.uni-hannover.de
51. Takahashi R et al. (the TAMA Collab.) *Class. Quantum Grav*. **25** 114036 (2008)
52. Tama, http://tamago.mtk.nao.ac.jp
53. LIGO, http://www.ligo.caltech.edu
54. Levin Yu *Phys. Rev D* **57** 659 (1998)
55. Bondu F, Hello P, Vinet J-Y *Phys. Lett. A* **246** 227 (1998)
56. Liu Y T, Thorne K S *Phys. Rev D* **62** 122002 (2000)
57. Braginsky V B, Gorodetsky M L, Vyatchanin S P *Phys. Lett. A* **271** 303 (2000)
58. Braginsky V B, Gorodetsky M L, Vyatchanin S P *Phys. Lett. A* **264** 1 (1999)
59. Yamamoto K et al. *Phys. Lett. A* **280** 289 (2001)
60. Ageev A Yu, Bilenko I A, Braginsky V B, Vyatchanin S P *Phys. Lett. A* **227** 159 (1997)
61. Ageev A Yu, Bilenko I A, Braginsky V B *Phys. Lett. A* **246** 479 (1998)
62. Abbott R et al. *Class. Quantum Grav*. **21** S915 (2004)
63. Gurkovsky A G, Strigin S E, Vyatchanin S P *Phys. Lett. A* **362** 91 (2007)
64. Gras S et al. *Class. Quantum Grav*. **27** 205019 (2010)
65. Yamamoto K et al. *J. Phys. Conf. Ser*. **122** 012015 (2008); arXiv: 0805.2385
66. Gurkovsky A G, Vyatchanin S P *Phys. Lett. A* **370** 177 (2007)
67. Hild S, Chelkowski S, Freise A, arXiv:0810.0604
68. Yamamoto K et al., http://www.et-gw.eu, Document ET-029-09 (2009)
69. Abernathy M et al., http://www.et-gw.eu, Document ET-0106A-10 (2011)
70. Strigin S E *Opt. Spektrosk*. **112** 414 (2012) [*Opt. Spectrosc*. **112** 373 (2012)]
71. D'Ambrosio E et al., gr-qc/0409075
72. O'Shaughnessy R, Strigin S, Vyatchanin S, gr-qc/0409050
73. Bondarescu M, Thorne K S *Phys. Rev. D* **74** 082003 (2006)
74. Bondarescu M, Kogan O, Chen Y *Phys. Rev. D* **78** 082002 (2008)
75. Mours B, Tournefier E, Vinet J-Y *Class. Quantum Grav*. **23** 5777 (2006)
76. Arlt J et al. *J. Mod. Opt*. **45** 1231 (1998)
77. Clifford M A et al. *Opt. Commun*. **156** 300 (1998)
78. Kennedy S A et al. *Phys. Rev. A* **66** 043801 (2002)
79. Courtial J, Padgett M J *Opt. Commun*. **159** 13 (1999)
80. O'Neil A T, Courtial J *Opt. Commun*. **181** 35 (2000)
81. Chu S-C, Otsuka K *Opt. Commun*. **281** 1647 (2008)
82. Chelkowski S, Hild S, Freise A *Phys. Rev. D* **79** 122002 (2009); arXiv:0901.4931
83. Strigin S E, Vyatchanin S P *Phys. Lett. A* **374** 1101 (2010)
84. Gras S, Blair D G, Ju L *Phys. Rev. D* **81** 042001 (2010)
85. Degallaix J et al. *J. Opt. Soc. Am. B* **24** 1336 (2007)
86. Ju L et al. *Class. Quantum Grav*. **26** 015002 (2009)
87. Miller J et al. *Phys. Lett. A* **375** 788 (2011)
88. Braginsky V B, Vyatchanin S P *Phys. Lett. A* **293** 228 (2002)
89. Zhao C et al. *Phys. Rev. A* **78** 023807 (2008)
90. Schliesser A et al. *New J. Phys*. **10** 095015 (2008); arXiv: 0805.1608
91. Schliesser A, Kippenberg T J *Adv. Atom. Mol. Opt. Phys*. **58** 207 (2010); arXiv:1003.5922
92. Matsko A B et al. *Phys. Rev. Lett*. **103** 257403 (2009)
93. Savchenkov A A et al. *Opt. Lett*. **36** 3338 (2011)
94. Bahl G et al. *Nature Commun*. **2** 403 (2011)